Hindawi
Advances in Civil Engineering
Volume 2020, Article ID 9384080, 16 pages
https://doi.org/10.1155/2020/9384080

Research Article

Infill Modelling Influence on Dynamic Identification and Model Updating of Reinforced Concrete Framed Buildings

Marco Bovo,[1] **Michele Tondi**,[2] **and Marco Savoia**[2]

[1]*DISTAL, Viale Giuseppe Fanin 48-40127, Bologna, Italy*
[2]*DICAM, Viale Risorgimento 2-40136, Bologna, Italy*

Correspondence should be addressed to Marco Bovo; marco.bovo@unibo.it

Received 3 December 2019; Revised 27 April 2020; Accepted 29 May 2020; Published 19 June 2020

Academic Editor: Flavio Stochino

In order to correctly capture the dynamic behavior of infilled framed buildings, the importance to take into account in seismic design the infill panels' contribution is nowadays well recognized since they could modify in a significant way the global and local response of the whole building. Despite about sixty years of continuous research in the field, the modelling of the frame-infill interaction still represents a serious issue for the daily practical design since there is no reference model proven to be suitable to cover a wide record of possible cases. Moreover, few works are available in the literature, comparing the results of different modelling proposals with outcomes of dynamic tests on a full-scale building. To this regard, starting from the results of induced vibration dynamic tests performed on a 7-story building with reinforced concrete frames with masonry infill, in the present paper, the effects of the infill presence have been evaluated by comparing experimental outcomes, achieved using a MDOF Circle-Fit identification procedure, with the results obtained by means of numerical analyses performed on finite element models. Using a model updating procedure, the optimal width to assign to the masonry equivalent struts modelling the infill panels was defined. Furthermore, several literature proposals for the definition of the equivalent strut width have been analysed. Thirteen different proposals have been selected and implemented in thirteen different finite element models. The reliability of each proposal has been investigated and quantified by comparing the dynamic properties of the models with the building dynamic response obtained by the experimental tests. The main outcomes of the analyses highlight that different proposals provide a great variability for the strut width. This brings to a large variability of the mechanical properties of the equivalent struts, and as a consequence, the modelling choice also influences the dynamic behaviour of the numerical models. Currently, this represents a serious issue for the daily designers' activity. The outcomes provided in the paper, although established for a specific case study, can be extended to a wide range of buildings and should drive the future research studies in order to provide more robust criteria for the modelling of this worldwide building class.

1. Introduction

The study of frame-infill panel interaction started since the early sixties, and it still represents an open issue. Only with a proper interpretation of the interaction between infill panels and surrounding frames, it is possible to achieve the correct comprehension of the behavior of a building under horizontal dynamic loading [1]. As far as reinforced concrete (RC) frames infilled by masonry panels are concerned, the interaction between infill and frames plays an important role for the design of new buildings and for the seismic assessment of the existing ones. Actually, several experimental campaigns showed that frame-infill interaction can produce an important modification to the whole system stiffness [2–7], and also the force distribution in the frame elements (i.e., beams and columns) can vary significantly if compared to the case of the bare frame [8].

In the last sixty years, a lot of researchers worked on the definition of modelling criteria in order to take into account the infill contribution. Following the consolidated literature [8, 9], the different numerical models could be classified into micro-, meso-, and macromodels. Macromodels are the most used models in applications requiring the modelling of an entire building [10]. The macromodels

proposed by researchers in order to reproduce the frame-infill interaction are, almost all, based on the concept of equivalent struts [8–10], i.e., two diagonal finite elements having only axial stiffness and simulating the presence of the infill panels.

Polyakov [11], among the first, modelled the infilled masonry panels as a diagonal strut with axial stiffness only. Then, Stafford Smith [12] refined the models by introducing a dimensionless parameter λ_h in order to take into account the relative stiffness between the panel and the surrounding frame (see also [13–15]). An alternative expression in order to consider the frame-infill panel relative stiffness was introduced by Bazan and Meli [16]. Hendry [17] proposed to evaluate and consider, in the definition of the equivalent strut, both the infill column and infill beam contact length. Paulay and Priestley [18] proposed a constant value set equal to 0.25, for the strut width (w) and diagonal panel length (d) ratio. Durrani and Luo [19] refined furtherly the proposal with the introduction of the two parameters γ and m. Recently, the influence of the vertical load on the panel-frame contact length was experimentally tested and numerically analysed by Cavaleri et al. [1], Amato et al. [20], and Campione et al. [21], suggesting expressions for the w/d ratio that explicitly consider the vertical load value.

In the present paper, starting from the experimental results collected during tests on a multistory building selected as a case study, a numerical finite element (FE) model was calibrated with the aim of identifying the contribution of the infill panels to the dynamic behavior of a real building. The selected structure, located in Reggiolo (Reggio Emilia, North-East of Italy), is depicted in Figure 1. The building has been designed according to the Italian building code D.M. 27/07/1985 [22] and has been built in 1990 with the bearing system constituted by RC frames infilled by stiff panels of hollow clay blocks. After some inspections and a detailed geometrical survey of the building, preliminary characterization tests (i.e., compression tests on concrete cored samples, tensile tests on steel reinforcement bars, and double flat-jack tests on masonry panels) were performed in order to obtain the main mechanical properties of the materials. Then, by means of dynamic excitation tests with a vibration generator, the natural frequencies and the mode shape components have been obtained.

In the second part of the paper, a model updating procedure has been adopted using a single equivalent diagonal strut replacing the infill panels, in order to capture the global behavior of the structure. In this way, the numerical calibration phase requires the updating of only one parameter (i.e., the width w of the equivalent strut). By means of the FE models, a parametric analysis has been carried out, varying the width w of the equivalent strut from zero (i.e., absence of infill) to the value 0.40 d, where d represents the diagonal panel length. By comparing the obtained frequencies and mode shape components, respectively, from the numerical model and experimental tests, it was possible to define a reliable w/d value. Then, the effects of considering or excluding the building basement (i.e., the underground story) was studied.

Figure 1: External view of the case study building.

Lastly, in order to evaluate the effectiveness of different literature proposals for the calibration of the equivalent strut dimensions, a comparison between the dynamic response of the building adopting these proposals and the optimal solution obtained through the parametric analysis was set. The main outcomes of the analyses highlight that different existing proposals provide a range of w/d values affected by great variability. All of this brings to a large variability of the mechanical properties that equivalent struts will assume by adopting a proposal rather than another one, but as a consequence, the choice will also influence the dynamic behaviour of the FE model implementing those struts. Currently, this represents a serious issue for the daily designers' activity. The outcomes provided in the paper, although established for a specific case study, can be extended to a wide range of buildings and should drive the future research studies to provide more robust criteria for the modelling of this worldwide building class.

2. Description of the Case Study

The case study is a 6-story building aboveground with a further basement story. The building has commercial units at the ground floor and residential dwellings at the upper floors. Garages are located in the basement. The building has a floor surface of about 440 m^2 and a total height of about 20 m above the ground level. The building has RC bearing frames and stairwell and lift at the center of the plan, in a vertical tube structure with a 20 cm thick RC walls. The columns have 30×45 cm cross section at the underground and ground floor and 25×30 cm at the other floors. The beams have a rectangular section at all stories except the second one having perimeter L-shaped beams. The stories have a stiff RC slab. The foundation elements are reverse T-shaped RC beams. The infill panels are constituted by brickwork with hollow clay blocks and concrete mortar. The perimeter walls are 30 cm thick, while the partitions are 25 cm thick. From the building inspections, it was emerged

that there are no connectors between infill walls and RC frames.

The vertical loads, deduced by the original design documentation, were modified based on the outcomes of the detailed survey. The uniformly distributed vertical loads considered in numerical analysis are 4.34 kN/m^2, 4.48 kN/m^2, and 3.85 kN/m^2, respectively, for the first story, stories from two to six, and the roof story. Only dead loads have been considered because when dynamic excitations have been induced in the structure, the building was not used and no live loads were present. In order to consider in a properly way the masses and stiffness of the infill walls in the FE models, they were modelled in their position, considering a specific weight for the masonry equal to 12 kN/m^3.

3. Experimental Campaign

3.1. Mechanical Characterization of the Material Properties. With the aim of characterizing the material properties of RC columns and walls, preliminary experimental investigations were conducted on vertical elements. 21 RC drilled core samples were collected in situ. The outcomes emerged from compressive tests provide an R_{ck} (i.e., characteristic cubic strength) value of 40 MPa for the underground and ground story and 30 MPa for structural elements of other stories. Moreover, by means of four double flat-jack tests on masonry panels, an average Young modulus $E = 2995$ MPa and an average compressive strength $f_m = 3.85$ MPa have been obtained for the infill panels.

3.2. Dynamic Excitation Tests. With the aim of identifying the main dynamic characteristics of the structure, experimental dynamic tests with induced vibrations were performed. The vibration generator was anchored to the roof floor (story #7) close to a symmetry axis (in the direction NW-SE in the global reference system as depicted in Figure 2). The vibration generator is a machine that, firmly anchored to the structure, allows the application of forces that vary over time with the sinusoidal law. It basically consists of two counter-rotating discs around two parallel rotation axes; two masses are constrained to each disk whose relative position is identified by the angle α formed by the joints joining their center of gravity with the axis of rotation. The maximum intensity of the applied force, depending on the mechanical parameters indicated by the manufacturer of the vibration inducer (ISMES, Bergamo, Italy), was 22 kN. Two test phases, associated with two different directions of the vibration generator (Position #1 and Position #2), have been considered. With the vibration generator in Position #1, horizontal forces in the direction NW-SE were applied. With the vibration generator in Position #2 (i.e., 90° rotated with respect to the former), horizontal forces in the direction NE-SW were induced. For convenience reasons, a local reference system with axes x and y in directions NE-SW and NW-SE, respectively, was defined (see Figure 2). In the various positions where the vibration generator is placed, the frequency range deemed of interest for assessing the dynamic behavior of the structure was explored with different values of the force intensity, corresponding to different values of the relative angle between the masses α.

The instrumentation used to record the acceleration during the tests was constituted by 12 piezoelectric accelerometers PCB/393B12 (labelled in the following as A1–A12) with a sensitivity equal to 10 volt/g. The position of the accelerometers is depicted in Figure 2 in both plan and elevation views. Furthermore, Figure 3 depicts some details relative to the positioning of the vibration generator on the roof and some connection details of the accelerometers on the walls of the structure.

3.3. Dynamic Identification Procedure. The natural frequencies of the building were identified as the peak values of the inertance function. The mode shape components were obtained by the peak values of the modulus and the phase of the inertance function of each accelerometer in correspondence with the peaks itself using a standard MDOF Circle-Fit procedure [23–25]. The mode shape components recorded for each identified mode shape are reported for Position #1 and Position #2 in Tables 1 and 2, respectively. The identified frequencies range from 2.55 Hz to 9.62 Hz for Position #1 and from 2.47 Hz to 9.57 Hz for Position #2.

Figure 4 shows, for the sake of brevity, the dominant natural vibration modes identified for the structure. The identified modes were the first flexural modes in the two directions (associated to the frequencies 2.47 Hz and 2.55 Hz), two torsional modes (with a frequency of about 2.75 Hz and 8.98 Hz), and the second prevailing flexural modes in the two directions (having frequencies of 18.55 Hz and 21.71 Hz).

4. Literature Proposals for Infill Modelling

In the literature studies focused on infill-frame interaction, the attention of researchers was mainly devoted to the definition of numerical models able to reliably simulate the global behavior of the whole system. In the present study, only macromodels have been considered because micro- and mesomodelling, typically used for analysis of single infill panels or small building portions [10], are computationally very expensive and not suitable for the study of a whole building. The macromodels proposed by researchers in order to reproduce the frame-infill interaction are, almost all, based on the concept of equivalent struts [8–10], but a further subclassification can be based on the number of equivalent struts adopted for the infill modelling. Crisafulli et al. [8] showed that equivalent single-strut models are not suitable to represent the stress distribution in the RC frame, and if these stresses are required, multistrut models must be considered. A detailed description and applications of multistrut models can be found in [26–29]. On the other hand, Asteris et al. [10] showed that single-strut models provide reliable approximations of the global response of the structures, as, for example, the definition of the mode shape components and natural frequencies of a building (see also [7, 30, 31]). Hence, in the present paper, only single-strut models were considered, being the work focused on the global behavior of the whole building.

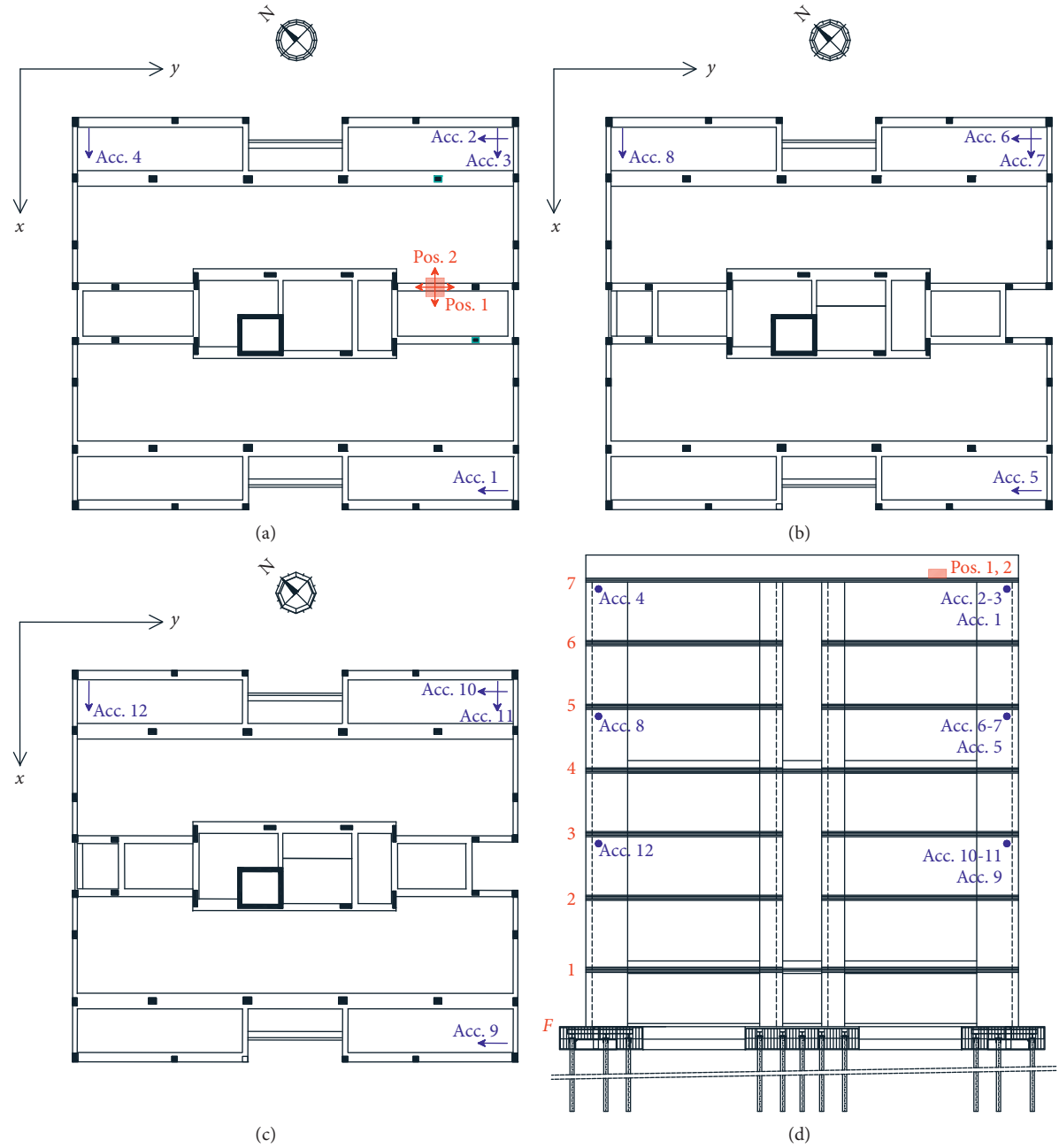

FIGURE 2: Positions of accelerometers and the vibration generator during the dynamic tests. (a) Plan view of floor #7 (roof floor); (b) plan view of floor #5; (c) plan view of floor #3; (d) vertical section of the building.

Following the approach of Polyakov [11], several researchers studied the issue at hand, by modelling the infilled masonry panels as a diagonal strut with axial stiffness only. The literature evaluated in the present paper provides different methodologies and expressions in order to define the equivalent strut width (w) to be multiplied for the panel thickness (t) in order to obtain the gross cross-sectional area of the diagonal strut, whereas the elastic modulus E adopted for the equivalent strut is that of the masonry itself. Table 3 collects the different proposals, from various authors, considered in the present work for the definition of the w/d ratio. Some authors have proposed specific parameters to take into account the particular aspects in their proposals. The most widespread parameters are reported in Table 4. For example, the dimensionless λ_h parameter, introduced by Stafford Smith [12] and then adopted in several other works [13–15], is defined in the following way:

$$\lambda_h = \sqrt[4]{\frac{E_m \cdot t \cdot \sin(2\theta)}{4E_c \cdot I_c \cdot h_m}} \cdot h, \tag{1}$$

where t and h_m are, respectively, the thickness and height of the panel; E_m and E_c are, respectively, the Young modulus of masonry and Young modulus of concrete; θ is the slope of the diagonal of the panel with respect to the horizontal plane;

(a)

(b)

Position	Series	α	Investigated frequency ranges (Hz)	Force ranges (kN)
1	AA	46°	1.0/4.6	0.94/19.99
1	BB	120°	3.6/6.4	6.64/21.01
1	CC	160°	6.0/10.8	6.41/20.78
1	DD	172°	10.4/17.2	7.74/21.17
1	EE	174°	15.8/19.5	13.40/20.41
2	FF	46°	1.0/4.6	0.94/19.99
2	GG	120°	4.0/6.3	8.21/20.36
2	HH	160°	6.0/10.8	6.41/20.78
2	II	176°	10.4/23.4	3.87/19.60

(c)

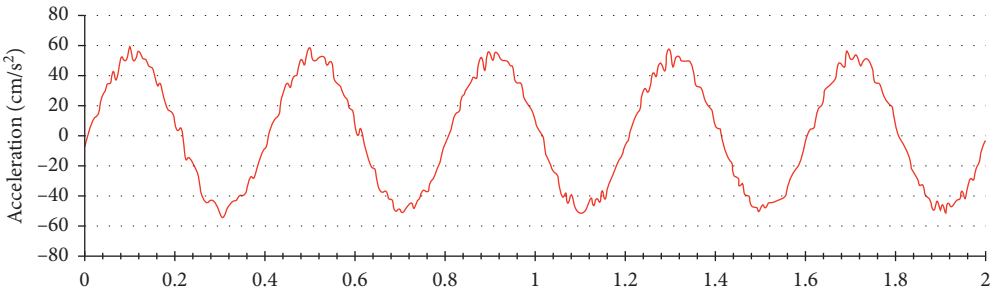

(d)

Figure 3: Instrumentation adopted during dynamic tests. (a) View of floor #7 with the vibration generator in Position #1. (b) Detail of the positioning of accelerometers A3 and A4. (c) Frequency ranges investigated with the vibration generator (extracted from the test report). (d) Example of acceleration time history recorded by the accelerometer A4 during the series FF, for an excitation frequency equal to 2.5 Hz.

I_c is the moment of inertia of the columns; h is the height of the columns.

In addition, to take into account the infill-frame contact length (z) in the w/d evaluation, Stafford Smith [12] proposed the following expression:

$$\frac{z}{h} = \frac{\pi}{2\lambda_h}, \tag{2}$$

where h represents the height of the columns.

An alternative formulation to evaluate the frame-infill relative stiffness has been proposed by Bazan and Meli [16], through the definition of the dimensionless parameter β:

$$\beta = \frac{E_c \cdot A_c}{G_m \cdot A_m}, \tag{3}$$

where A_c is the gross cross-section area of the columns, A_m is the area of the horizontal section of the infill panel (panel length × panel thickness), and G_m is the shear modulus of the panel. Hendry [17] proposed to evaluate separately the panel-beam relative stiffness (λ_b) from the panel-column relative stiffness (λ_c) with the following expressions:

$$\lambda_b = \left[\frac{E_m \cdot t \cdot \sin(2\theta)}{4E_c \cdot I_b \cdot h_m}\right]^{(1/4)}, \tag{4}$$

$$\lambda_c = \left[\frac{E_m \cdot t \cdot \sin(2\theta)}{4E_c \cdot I_c \cdot h_m}\right]^{(1/4)}. \tag{5}$$

Table 1: Natural vibration modes identified by dynamic tests with the vibration generator in Position #1.

Mode	f (Hz)	A1	A2	A3	A4	A5	A6	A7	A8	A9	A10	A11	A12
1	2.55	1.00	0.34	0.40	—	0.76	0.24	0.32	—	0.53	0.12	0.21	—
2	2.75	1.00	−0.63	0.90	—	0.79	−0.54	0.78	—	0.59	−0.39	0.54	—
3	8.98	−0.92	−0.60	−0.19	—	0.17	0.16	0.02	—	1.00	0.67	0.19	—
4	9.62	−0.69	1.00	−0.81	—	−0.01	−0.05	0.02	—	0.68	−0.97	0.83	—
5	18.71	—	—	−0.02	−0.00			1.00	0.00	−0.12	0.00	0.00	0.45

Natural frequency and components of the modal eigenvectors for each of the 12 accelerometers A1–A12 (columns) and for each of the five identified modes (rows).

Table 2: Natural vibration modes identified by dynamic tests with the vibration generator in Position #2.

Mode	f (Hz)	A1	A2	A3	A4	A5	A6	A7	A8	A9	A10	A11	A12
1	2.47	0.00	0.06	0.88	1.00	0.00	0.05	0.71	0.81	0.00	0.06	0.44	0.49
2	2.79	−0.66	0.80	−0.72	1.00	−0.55	0.70	−0.63	0.85	−0.42	0.50	−0.47	0.56
3	8.66	−0.31	0.06	−0.89	−0.29	0.03	0.01	0.16	0.11	0.37	−0.13	1.00	0.36
4	9.57	−0.78	0.70	−0.64	1.00	0.03	0.00	0.01	−0.08	0.76	−0.65	0.65	−0.92
5	18.55	0.39	−0.64	0.33	0.78	1.00	−0.94	0.58	0.04	0.46	−0.40	0.24	0.56
6	21.71	1.00	0.03	0.00	−0.01	−0.03	0.04	0.01	−0.03	−0.04	0.04	0.03	−0.03

Natural frequency and components of the modal eigenvectors for each of the 12 accelerometers A1–A12 (columns) and for each of the five identified modes (rows).

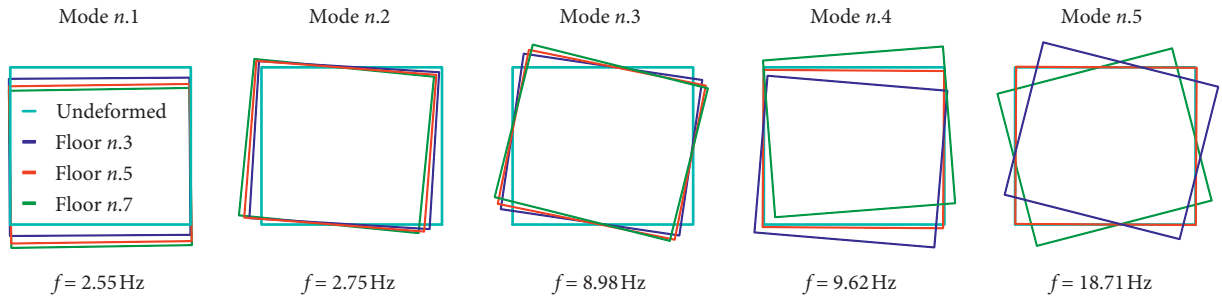

Figure 4: Natural vibration modes experimentally identified.

Analogously, the panel-beam contact length (z_b) and the panel-column contact length (z_c) are computed with the following expressions:

$$z_b = \frac{\pi}{2\lambda_b}, \tag{6}$$

$$z_c = \frac{\pi}{2\lambda_c}. \tag{7}$$

Durrani and Luo [19] proposed to evaluate the relative stiffness panel-frame as reported in the following equation:

$$\gamma = 0.32\sqrt{\sin(2\theta)}\left(\frac{h^4 \cdot E_m \cdot t}{m \cdot E_c \cdot I_c \cdot h_m}\right)^{-0.1}, \tag{8}$$

by means of the m coefficient reported in the following equation:

$$m = 6 \cdot \left(1 + \frac{6E_b \cdot I_b \cdot h}{\pi \cdot E_c \cdot I_c \cdot L}\right). \tag{9}$$

Recently, a panel-frame relative stiffness parameter (λ^*) was proposed by Papia and Cavaleri [40] and Papia et al. [41]:

$$\lambda^* = \frac{E_m}{E_c} \cdot \frac{t * h'}{A_c} \cdot \left(\frac{h'^2}{l'^2} + \frac{1}{4} \cdot \frac{A_c}{A_b} \cdot \frac{l'}{h'}\right), \tag{10}$$

where A_b is the beam gross cross-section area, l' is the length of the beam measured between the centrelines of the columns, and $h\prime$ is the height of the columns measured between the centrelines of the beams.

Furthermore, recently, the influence of the vertical load value on the panel-frame contact length was experimentally tested and numerically analysed by Cavaleri et al. [1], Amato et al. [20], and Campione et al. [21], suggesting expressions for the w/d ratio that explicitly consider the vertical load value.

5. Model Updating

5.1. Finite Element Modelling. For the investigated building, an FE model has been achieved by means of the software SAP2000 [42]. The frame elements were modelled through mono-dimensional linear elastic Timoshenko beam/column elements. The RC walls of the underground story and the lift tube were modelled with classic bidimensional linear elastic 4-node Reissner–Mindlin shell elements. The base nodes have been

Table 3: Expressions proposed in literature for the evaluation of the w/d ratio (see [9]).

Authors (year)	Proposed expression	Notes
Holmes (1961) [32]	$w/d = 1/3$	$\lambda_h < 2$
Stafford Smith (1967) [14]	$0.10 < w/d < 0.25$	The value depends on λ_h
Mainstone (1971) [33]	$w/d = 0.16\lambda_h^{-0.3}$	For λ_h, see equation (1)
Mainstone (1974) [34]	$w/d = 0.175\lambda_h^{-0.4}$	Adopted by FEMA-274 [35] and FEMA-306 [36]
Bazan and Meli (1980) [16]	$w = (0.35 + 0.022\ \beta)\ h_m$	$0.9 \le \beta \le 11$; for β, see equation (3)
Hendry (1981) [17]	$w = 1/2\sqrt{z_b^2 + c_c^2}$	For z_b and z_b, see equations (6) and (7)
Tassios (1984) [37]	$w/d = 0.20\ \beta\ \sin\theta$	$1 \le \beta \le 5$
Te-Chang and Kwok-Hung (1984) [38]	$(w/d) = (0.95 \sin(2\theta)/\sqrt[3]{\lambda_h})$	$25^\circ \le \theta \le 50^\circ$
Decanini and Fantin (1987) [39] for uncracked panels	$(w/d) = 0.085 + (0.748/\lambda_h)$ $(w/d) = 0.130 + (0.393/\lambda_h)$	For $\lambda_h \le 7.85$ For $\lambda_h > 7.85$
Decanini and Fantin (1987) [39] for cracked panels	$(w/d) = 0.010 + (0.707/\lambda_h)$ $(w/d) = 0.040 + (0.470/\lambda_h)$	For $\lambda_h \le 7.85$ For $\lambda_h > 7.85$
Paulay and Priestley (1992) [18]	$w/d = 0.25$	For $\lambda_h < 4.00$
Durrani and Luo (1994) [19]	$w/d = \gamma\ \sin(2\theta)$	For γ, see equations (8) and (9)
Cavaleri et al. (2005) [1] Amato et al. (2008) [20]	$(w/d) = (k/z \cdot c/(\lambda^*)^\beta)$	In which, coefficients c and β take into account the Poisson ratio; k takes into account the vertical load; z is a geometrical parameter; λ^* is a parameter depending on the elastic and the geometric features of the system

fully restrained. The stories were considered as rigid diaphragms in their plane because of the presence of the RC slabs.

The geometric properties of elements have been deduced by a detailed survey of the structure. The material properties have been obtained from the experimental characterization tests. An elastic modulus E_c equal to 35030 MPa has been assigned to RC elements in the underground and the ground story, while a modulus equal to 29994 MPa has been used for the elements in the upper stories.

The infill panels have been modelled through an equivalent single strut for each diagonal with only axial stiffness. The Young modulus of masonry has been assumed to be equal to $E_m = 2995$ MPa. The elastic material properties adopted in the FE models are summarized in Table 4. The infill panels inserted in the model have been the perimeter walls (30 cm thick) and the partitions (25 cm thick). The stiffness has been reduced by means of proper reduction factors to take into account the opening presence [43]. With the aim to not introduce in the model a double strut stiffness, due to the presence of a strut for each diagonal, a value equal to one-half of the real thickness has been introduced in the FE model. The structural model obtained is depicted in Figure 5. In order to define the more suitable width w for the equivalent struts, the model updating process described in the following section has been adopted.

Finally, in order to obtain the numerical natural frequencies and mode shape components, to compare with the experimental outcomes, modal decomposition analyses have been performed on the FE models of the building.

5.2. Definition of Target Function H. In order to investigate the effects of the infill panels' presence on the dynamic behavior of the building, a parametric study was performed by varying the w/d ratio in the range 0.0–0.40.

For each considered w/d value, natural frequencies and mode shape components of the building have been recorded. Then, matching between numerical and experimental outcomes was checked through a target function H defined as follows:

$$H = \sum_{i=1}^{N}\left[w_{1i}\left(\frac{\omega_i - \overline{\omega}_i}{\overline{\omega}_i}\right)^2 + w_{2i}\mathrm{NMD}_i^2\right], \tag{11}$$

where N represents the number of eigenmodes, w_{1i} and w_{2i} are the two weight functions, and NMD_i (normalized modal difference) is defined as follows [25]:

$$\mathrm{NMD}_i = \sqrt{\frac{1 - \mathrm{MAC}(\varphi_i, \overline{\varphi}_i)}{\mathrm{MAC}(\varphi_i, \overline{\varphi}_i)}}. \tag{12}$$

The H function represents the relative error between frequencies and mode shape components obtained via the FE model (ω_i, φ_i), for a fixed set of parameters, and the same quantities obtained experimentally ($\overline{\omega}_i$, $\overline{\varphi}_i$). The modal assurance criterion (MAC) represents a parameter ranging between 0 and 1. It is used in order to provide indications on the matching between numerical and experimental mode shapes (e.g., MAC close to 1 indicates that two modes are very similar). The following expression for the MAC has been assumed [23, 44]:

$$\mathrm{MAC}(\varphi_i, \overline{\varphi}_i) = \frac{\left(\sum_{r=1}^{N_0}(\varphi_{ir} * \overline{\varphi_{ir}})\right)^2}{\sum_{r=1}^{N_0}\varphi_{ir}^2 * \sum_{r=1}^{N_0}\overline{\varphi_{ir}^2}}, \tag{13}$$

where N_0 represents the dimension of the analysed vectors.

The MAC parameters, collected in a histogram matrix form, result in a useful tool to identify the fitting between numerical and experimental modes.

By means of the dynamic excitation tests on the building, frequencies and mode shape components reported in Table 5 were identified. In the model updating process, N (number of modes) and N_0 (number of components) parameters were set to 5 and 12, respectively. The weight functions w_{1i} is defined as follows [25]:

Table 4: Elastic properties of the materials assumed in the FE models.

Material	Young modulus E (MPa)	Poisson ratio ν
Concrete in underground and ground story	35030	0.20
Concrete in the upper story	29994	0.20
Masonry for infill panels	2995	0.25

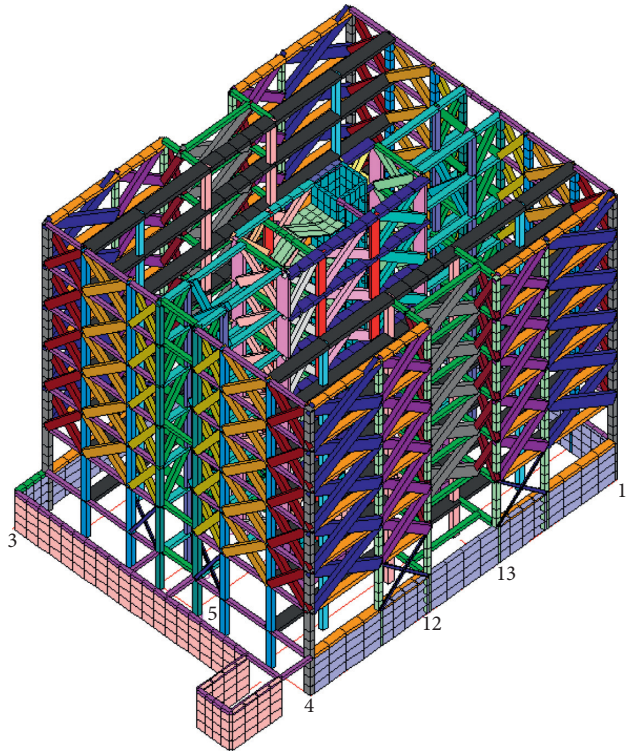

Figure 5: Geometry of the case study. Solid view of the finite element model.

Table 5: Frequencies and mode shape components experimentally identified and used for the comparison with the FE model results.

Mode	f (Hz)	A1	A2	A3	A4	A5	A6	A7	A8	A9	A10	A11	A12
1	2.47	0.00	0.06	0.88	1.00	0.00	0.05	0.71	0.81	0.00	0.06	0.44	0.49
2	2.55	1.00	0.34	0.40	—	0.76	0.24	0.32	—	0.53	0.12	0.21	—
3	2.79	−0.66	0.80	−0.72	1.00	−0.55	0.70	−0.63	0.85	−0.42	0.50	−0.47	0.56
4	8.66	−0.31	0.06	−0.89	−0.29	0.03	0.01	0.16	0.11	0.37	−0.13	1.00	0.36
5	9.57	−0.78	0.70	−0.64	1.00	0.03	0.00	0.01	−0.08	0.76	−0.65	0.65	−0.92

$$w_{1i} = \frac{W_i}{\sum_{j=1}^{5} W_j}, \tag{14}$$

where w_i is the participating mass of the i-th mode with the introduction of the further assumption:

$$\sum_{i=1}^{5} w_{1i} = 1. \tag{15}$$

For the weight function w_{2i}, two different values, associated with two different hypothesis, have been considered:

$$w_{2i} = 0, \tag{16a}$$

or in alternative

$$w_{2i} = 0.10 \times w_{1i}. \tag{16b}$$

With the first criterion, only the errors on frequencies (i.e., without any contribution of errors connected to mode shape components) have been considered in the evaluation of the target function H. Instead, by adopting the second hypothesis, even the error contribution of the mode shape components have been introduced in the evaluation of H. Therefore, H function was computed for

two specific pair of weight functions: $(w_{1i}; 0)$ and $(w_{1i}; 0.10 \times w_{1i})$.

6. Results and Discussion

6.1. Determination of the Optimal w/d Ratio. The FE model considered in the study has been firstly analysed by considering a strut width equal to $w = 0$ (i.e., bare frames without infill). In this case, the experimental frequencies of the structure result are greatly underestimated as shown in Figure 6 and Table 6, respectively, reporting the main frequencies and the MAC matrix for the case neglecting the infill presence.

The H function, considering and excluding the mode shape contribution, assumes the value of 0.354 and 0.310, respectively. Obviously, it is worth noting that the model neglecting the infill presence does not match with the experimental outcomes, providing numerical frequencies very far from the experimental ones. Afterwards, the infill stiffness contribution has been introduced in the model as equivalent strut elements, and 40 different FE models have been analysed by considering 40 w/d values. Figure 7 depicts the evolution of the MAC matrix for some w/d ratios. For low w/d values, the MAC matrix results are sparse, and only three experimental modes are adequately captured by the numerical model. By increasing the w/d ratio, the matrix tends to stabilize, and for values greater than 0.20, it results are almost diagonal. The H function versus the w/d ratio has the trend as depicted in Figure 8. For both criteria, the minimum of H function is achieved for the w/d ratio equal to 0.24. For this specific value, the MAC matrix is reported in Table 7. For the sake of a fast comparison, numerical frequencies obtained for $w/d = 0.24$ and experimental ones are reported in Table 8.

When suitable w/d values are introduced in the model, the four main frequencies (i.e., frequencies #1, #3, #4, and #5 with the highest mode participating factors) can be identified with high MAC values. With regard to the second mode, instead, a low MAC value has been obtained. This is probably because the second and the third experimentally identified modes have frequencies very close between them, respectively, 2.55 Hz and 2.79 Hz, and the related mode shapes are both characterized by a torque-bending coupling behavior. So, in order to capture these particular features of the real structure, a deep knowledge of the building details is necessary (e.g., the real distribution and position of masses over the floor, the role of the floor openings, and the role of infill openings). Furthermore, it is very complex to take into account some of these aspects in a numerical model since they can be considered as modelling uncertainties. Anyway, by adopting the value $w/d = 0.24$, which minimizes the H function, all numerical frequencies, with the exception on the second one, match very well with the experimental outcomes with the largest frequency error resulting lower than 10%.

6.2. FE Model without Underground Story. In order to numerically evaluate the effects of the presence of the underground story, a different FE model has been created excluding the underground story and introducing a full restraint at the base of the columns of the ground level. This model produces results altogether similar to the previous one, for every w/d value. This effect was expected because, in the experimental mode shapes, the deformation contribution of the underground story resulted almost negligible due to the considerable stiffness of the RC perimeter walls of the basement. Figure 9 and Table 9 show, as representative instance, results provided by the model without the underground story for $w/d = 0.24$. By comparing Tables 8 and 9, it appears clearly that the underground floor, because of its stiffness, does not influence the dynamic behavior of the building.

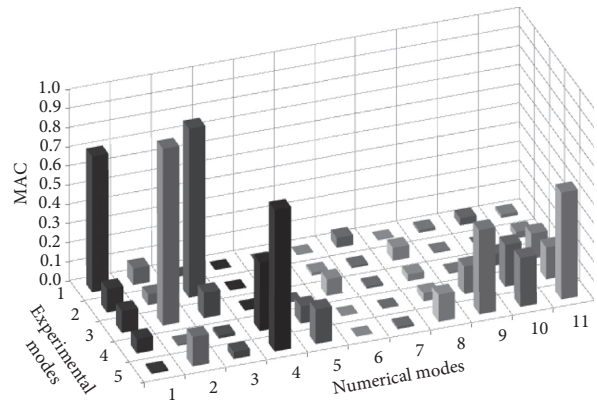

Figure 6: Model without equivalent struts: histogram representation of the MAC matrix.

6.3. Comparison between FE Models Adopting w/d Ratio Suggested by the Literature. Several expressions for the w/d ratio have been provided from the scientific literature, and some of them have been reported in the previous sections. In order to evaluate the agreement and the applicability of the different proposals to full-scale buildings, 13 different proposals have been selected and used for the generation of a specific FE model adopting the w/d ratio. The H values, obtained by considering the w/d ratio provided by the 13 selected proposals, are collected in Table 10 and shown in Figure 10. For the sake of comparison, in the table and in the figure, the H values obtained from the model with $w/d = 0.24$ have been also reported.

From the analysis of the different models, it emerges that more recent proposals provide results that are generally similar between them and rather close to results obtained for $w/d = 0.24$. For the case at hand, considering for the evaluation of the target function H by only the natural frequencies, the model which produces the best result is the method proposed by Bazan and Meli [16]. It is worth noting that the study performed by Aniendhita and Data [45], which considers 14 different proposals for the w/d ratio, also indicates that Bazan and Meli is one of the models (i.e., is the second over a total of 14 analysed models) providing the best fitting with experimental tests. On the other hand, following the results by Aniendhita and Data [45], Holmes' method

Table 6: Results of modal decomposition analysis obtained not modelling the infill panels (bare structure only) and comparison with experimental outcomes.

Experimental modes	Numerical modes	$(W_i/\sum_{i=1}^{5} W_i)$	Experimental frequencies f_i^* (Hz)	Numerical frequencies f_i (Hz)	Percentage differences (%)	MAC (%)
1	1	0.47	2.47	0.99	−59.92	70.86
2	3	0.32	2.55	1.31	−48.63	88.29
3	2	0.15	2.79	1.09	−60.93	92.37
4	5	0.05	8.66	4.11	−52.54	31.11
5	4	0.01	9.57	3.39	−64.58	74.10

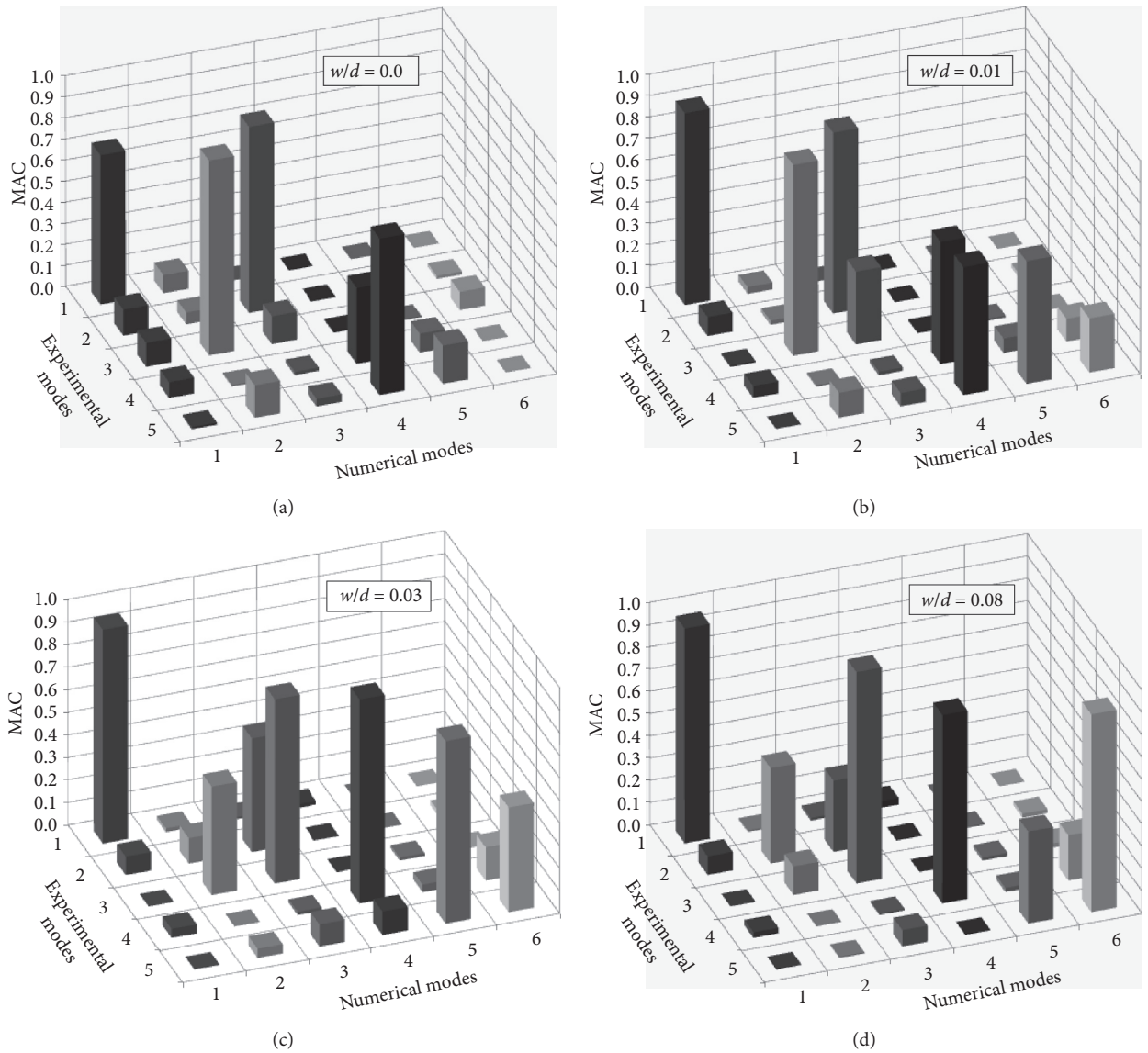

Figure 7: Continued.

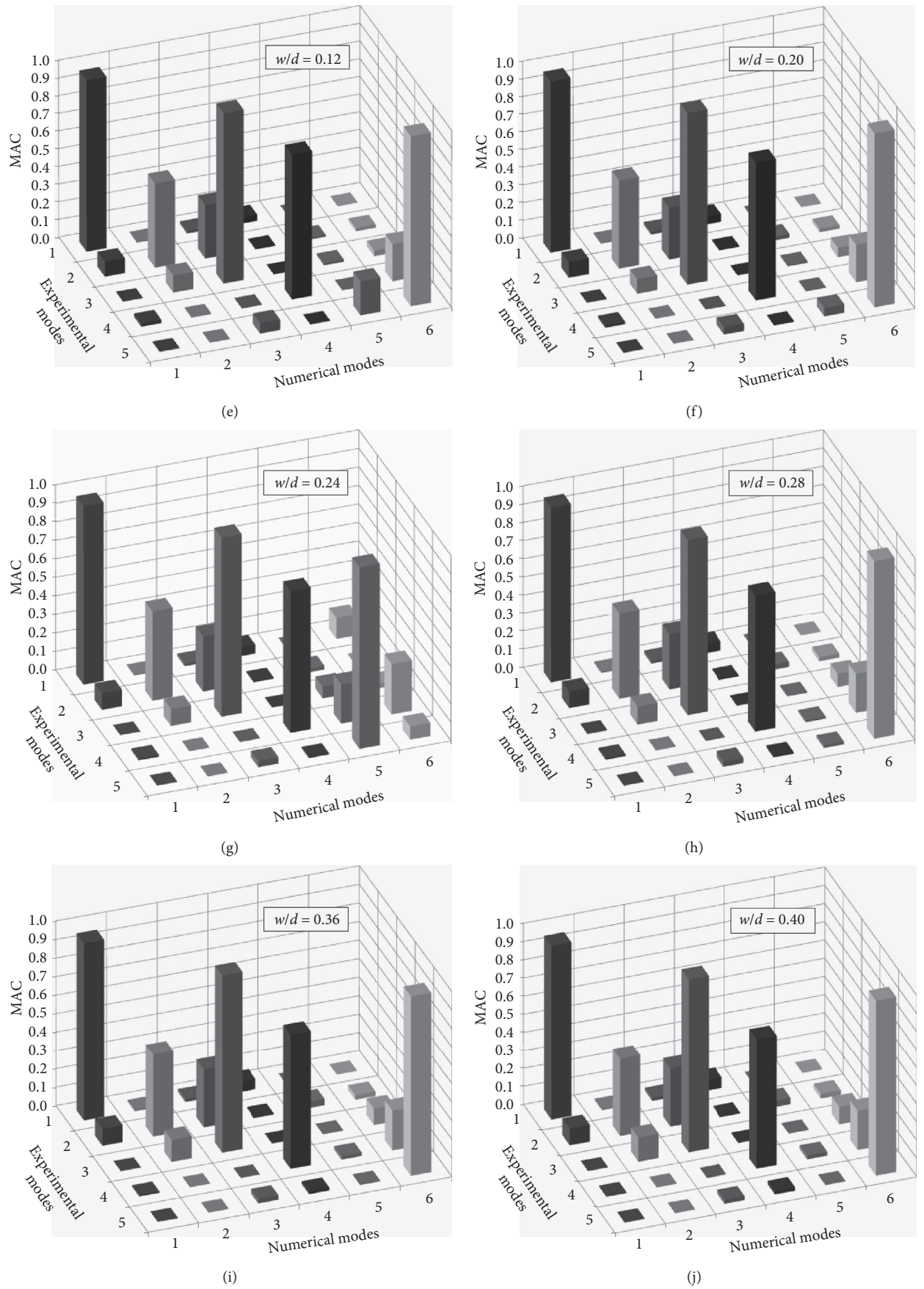

Figure 7: Evolution of the MAC matrix for w/d ratio ranging between 0.00 and 0.40.

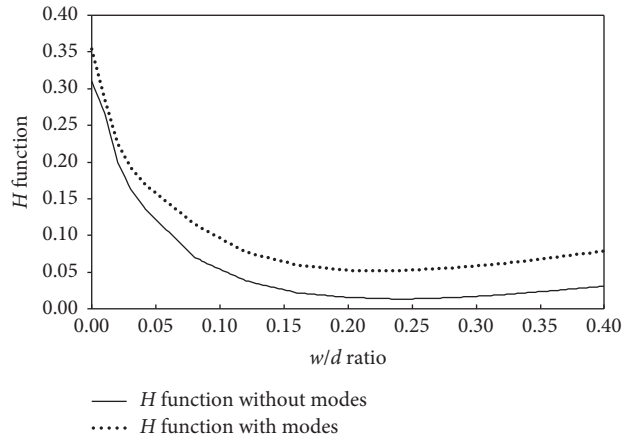

Figure 8: Target function H for the w/d ratio ranging between 0 and 0.40.

Table 7: MAC matrix (%) for $w/d = 0.24$.

		Experimental vibrating modes				
		1	2	3	4	5
Numerical vibrating modes	1	96.44	8.90	0.00	1.01	0.16
	2	0.53	48.21	9.15	0.11	0.11
	3	1.46	29.77	96.65	0.11	3.44
	4	4.68	0.55	0.03	76.41	0.62
	5	0.12	2.05	6.38	21.18	98.02
	6	11.23	0.11	2.60	27.22	7.20

Table 8: Results of the modal decomposition analysis assuming $w/d = 0.24$ and comparison with experimental outcomes.

Experimental modes	Numerical modes	$(W_i / \sum_{i=1}^{5} W_i)$	Experimental frequencies f_i^* (Hz)	Numerical frequencies f_i (Hz)	Percentage differences (%)	MAC (%)
1	1	0.46	2.47	2.19	−11.34	96.44
2	2	0.31	2.55	2.81	10.20	48.21
3	3	0.14	2.79	3.11	11.47	96.65
4	4	0.06	8.66	6.91	−20.21	76.41
5	5	0.03	9.57	9.62	0.52	98.02

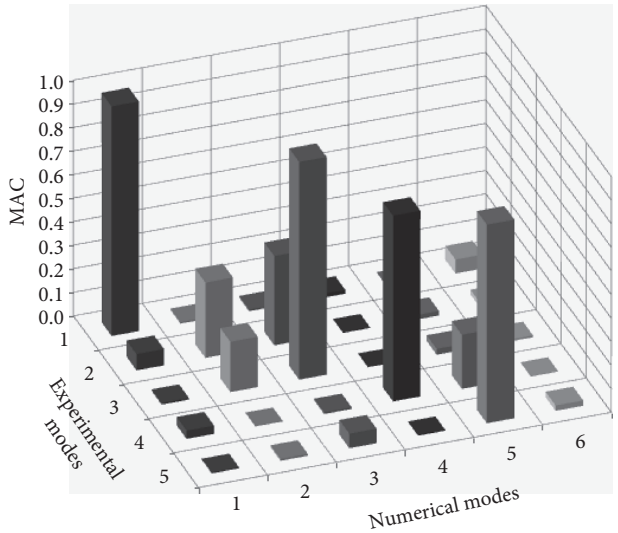

Figure 9: Model without the underground story: histogram representation of the MAC matrix for the optimal value of $w/d = 0.24$.

has the best performance, whereas in the present study, it provides an assessment of w/d far from the optimal value. Conversely, considering also the mode shapes in the H evaluation, the best fitting is obtained by the expression of Paulay and Priestley [18], providing a value of w/d ratio equal to 0.25, very close to the optimal value of 0.24.

For the case study investigated here, the comparison between the different literature proposals provided results for w/d with a similar order of magnitude but generally very different in values. In some cases, these results were also in disagreement with experimental evidence presented here.

Furthermore, it is useful to highlight how a correct prediction of the equivalent strut dimensions has a fundamental importance on the dynamic response of the numerical model. In fact, for the case studied here, it is possible to see how to adopt a model proposal rather than others which lead to w/d evaluations ranging from about 0.11 to 0.52, with the optimal value equal to 0.24. This means that the various existing proposals provide a range of w/d values affected by great variability. For the case studied here, they

Table 9: Results of the modal decomposition analysis from the model without the underground story, assuming $w/d = 0.24$, and comparison with experimental outcomes.

Experimental modes	Numerical modes	$(W_i/\sum_{i=1}^{5} W_i)$	Experimental frequencies f_i^* (Hz)	Numerical frequencies f_i (Hz)	Percentage differences (%)	MAC (%)
1	1	0.42	2.47	2.19	−11.34	97.51
2	2	0.29	2.55	2.77	8.63	31.97
3	3	0.17	2.79	3.01	7.89	92.40
4	4	0.08	8.66	6.85	−20.90	78.81
5	5	0.04	9.57	8.75	−8.57	84.25

Table 10: Values assumed by the target function H for models with equivalent struts defined using literature proposals and comparison with results obtained from the numerical model with a constant value of w/d ratio equal to 0.24.

Authors (year)	Function H evaluated without vibrating mode contribution	Function H evaluated with vibrating mode contribution
Holmes (1961) [32]	0.021	0.064
Stafford Smith (1967) [14]	0.022	0.069
Mainstone (1971) [33]	0.043	0.089
Mainstone (1974) [34]	0.046	0.095
Bazan and Meli (1980) [16]	0.010	0.058
Hendry (1981) [17]	0.037	0.073
Tassios (1984) [37]	0.029	0.098
Te-Chang and Kwok-Hung (1984) [38]	0.013	0.060
Decanini and Fantin (1987) [39] uncracked panels	0.019	0.091
Decanini and Fantin (1987) [39] cracked panels	0.014	0.086
Paulay and Priestley (1992) [18]	0.014	0.053
Durrani and Luo (1994) [19]	0.014	0.056
Cavaleri et al. (2005) [1] and Amato et al. (2008) [20]	0.017	0.059
Numerical model with $w/d = 0.24$	0.013	0.052

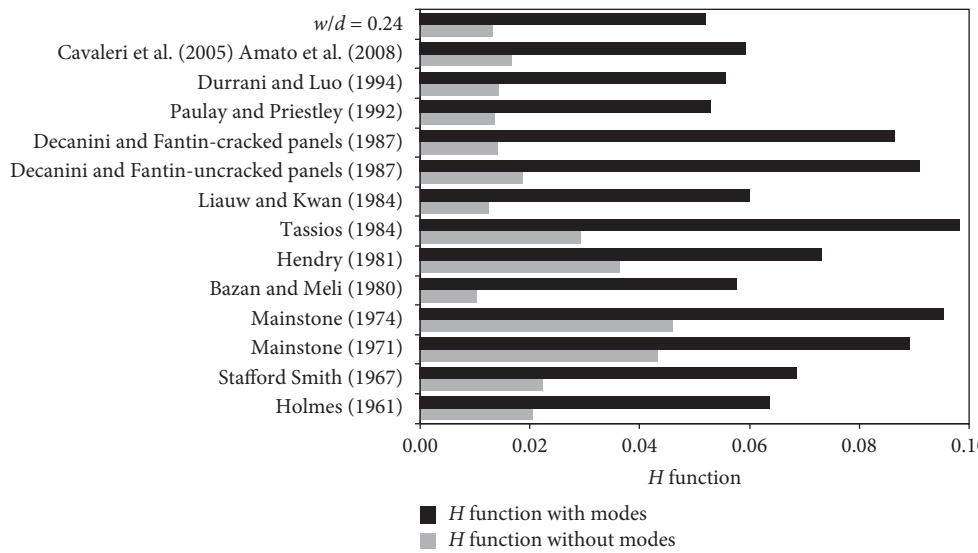

Figure 10: Target function histogram for the models with equivalent struts defined by literature proposals and comparison with model adopting a constant value of $w/d = 0.24$.

can vary from 46% (i.e., $0.11/0.24 \times 100$) to 217% ($0.52/0.24 \times 100$) of the optimal value. This entails large variability of the mechanical properties that equivalent struts will assume by adopting a proposal rather than another one, but, as a consequence, the choice will also influence the dynamic behavior of the FE model implementing those struts.

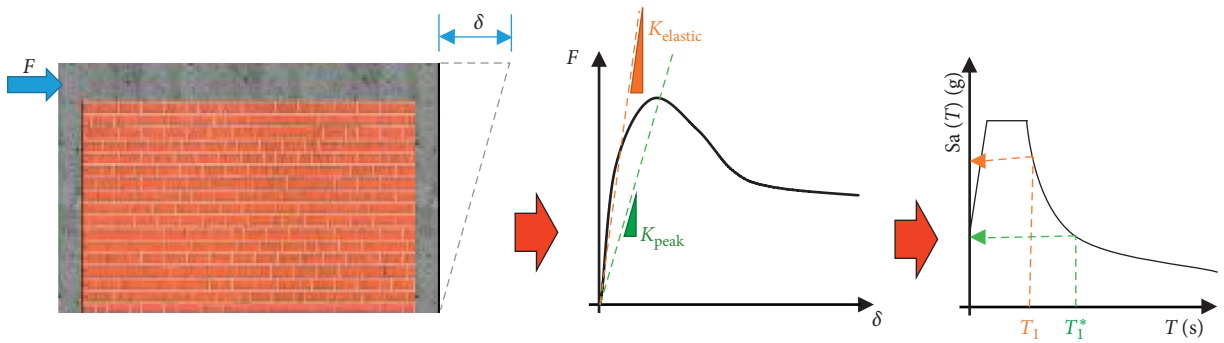

Figure 11: Consequences of nonsuitable assessment of the infill elastic stiffness in the everyday building seismic design.

Currently, this represents a serious issue for the daily designers' activity.

In addition, these models generally provided w/d evaluations lower than the required value for the optimal matching between experimental and numerical dynamic response, at least in the linear range (i.e., for low force values). This is because many of the proposals for w/d evaluation are based on the results of static tests in which the evaluation of the optimal w/d value is made by taking the peak strength of the nonlinear experimental force-displacement curve (see Figure 11).

This aspect, from a practical point of view, results in the clear possibility of underestimating the current elastic stiffness of the infill, and therefore leading to the definition of numerical models characterized by longer vibrating periods (T_1^* in Figure 11), generally affected by lower seismic actions. Obviously, all of this can be translated into a nonsafety assessment of the seismic state of the building.

Finally, it seems questionable if computation and modelling complications deriving from some very refined parameters as, for example, those connected to relative panel-frame stiffness or vertical loads acting on frame, are necessary for a reliable study of complex systems as real buildings. In fact, even for a more complex model, the introduction of those additional terms did not lead to significant improvements with respect to the simplified choice of adopting, in the FE model, the same equivalent strut width for all the infill panels of the building.

7. Final Remarks

The present paper describes the main results connected to dynamic identification and model updating of a building with RC frames infilled with masonry panels. As a first phase, experimental tests were carried out in order to properly characterize the mechanical properties of the materials. Then, dynamic tests with induced vibrations were performed in order to identify the natural frequencies and mode shape components. By means of numerical analyses, it was observed that only with the introduction of infill panels, it is possible to reproduce, with good approximation, the dynamic behavior of the whole structure.

By means of a parametric study, in which the w/d ratio (i.e., ratio between width and diagonal length of the equivalent axial strut modelling the infill panels) was used as a varying parameter, and an optimal value of the w/d ratio equal to 0.24 was identified for the case at hand. For this specific value, the target function, measuring the error between experimental and numerical quantities, assumes the minimum value and maximizes the matching between experimental and numerical dynamic response. This value has been then compared with values reported in the literature.

Furthermore, it has been observed that modelling or neglecting the basement of the building does not lead to substantial modification of both target function values and building dynamic behavior.

Finally, with the aim of measuring the accuracy of some literature proposals defining the w/d ratio, the original FE model has been modified, introducing diagonal struts as obtained by the application of 13 different expressions considered in the work. Comparing the results achieved by adopting the literature proposals with the experimental outcomes, the H function, computed considering only natural frequencies, resulted in a minimum value by adopting the Bazan and Meli's model [16], and the numerical results were in good agreement with the ones obtained with the model using a constant w/d ratio (equal to 0.24). This outcome is confirmed by similar works reported in the literature.

Conversely, the target function considering both frequencies and mode shape components presents the minimum value if the Paulay and Priestley's model [18] is used.

Moreover, from a practical point of view, different proposals provide very different values, ranging from 46% to 217% of the optimal value. This aspect, as a consequence, involves a large variability of the mechanical properties to be adopted in the FE modelling of buildings and could represent a serious issue for the daily practical design since this can lead the designer into nonsafety assessment of the seismic state of the building.

With reference to the case study building investigated here, it can be stated that most refined expressions, defining the w/d ratio, provide results substantially equal, and in some cases worse, with respect to a simpler model considering a constant w/d ratio for all masonry infill panels.

At the present state of the research, it seems that available literature proposals could provide an assessment of the optimal mechanical characteristics of the equivalent strut, but, for more refined evaluations, the building FE model that considers the presence of the infill should be updated based

on in situ experimental tests since the complex frame-infill interaction is strongly case dependent. These final remarks should drive the future studies to provide more robust criteria for the modelling of these very spread class of buildings.

Data Availability

No data were used to support this study.

Conflicts of Interest

The authors declare that there are no conflicts of interest regarding the publication of this paper.

Acknowledgments

The financial support of the Italian Department of Civil Protection (ReLUIS 2019 Grant-Innovative Materials) is gratefully acknowledged.

References

[1] L. Cavaleri, M. Fossetti, and M. Papia, "Infilled frames: developments in the evaluation of the cyclic behaviour under lateral loads," *Structural Engineering and Mechanics*, vol. 21, no. 4, pp. 469–494, 2005.

[2] A. Madan, A. M. Reinhorn, J. B. Mander, and R. E. Valles, "Modeling of masonry infill panels for structural analysis," *Journal of Structural Engineering*, vol. 123, no. 10, pp. 1295–1302, 1997.

[3] I. Koutromanos, A. Stavridis, P. S. Shing, and K. Willam, "Numerical modeling of masonry-infilled RC frames subjected to seismic loads," *Computers and Structures*, vol. 89, no. 11-12, pp. 1026–1037, 2011.

[4] B. Moaveni, A. Stavridis, G. Lombaert, J. P. Conte, and P. B. Shing, "Finite-element model updating for assessment of progressive damage in a 3-story infilled RC frame," *Journal of Structural Engineering*, vol. 139, no. 10, pp. 1665–1674, 2013.

[5] K. M. Mosalam and S. Gunay, "Progressive collapse analysis of reinforced concrete frames with unreinforced masonry infill walls considering in-plane/out-of-plane interaction," *Earthquake Spectra*, vol. 31, no. 2, pp. 921–943, 2015.

[6] M. Song, S. Yousefianmoghadam, M.-E. Mohammadi, B. Moaveni, A. Stavridis, and R. L. Wood, "An application of finite element model updating for damage assessment of a two-story reinforced concrete building and comparison with lidar," *Structural Health Monitoring*, vol. 17, no. 5, pp. 1129–1150, 2018.

[7] M. Tondi, S. Yousenfianmoghadam, A. Stavridis, B. Moaveni, and M. Bovo, *Model Updating and Damage Assessment of RC Structure Using an Iterative Eigenvalue Problem Dynamics of Civil Structures*, vol. 2, Springer International Publishing, New York, NY, USA, 1st edition.

[8] F. J. Crisafulli, A. J. Carr, and R. Park, "Analytical modelling of infilled frame structures—a general review," *Bulletin of the New Zealand Society for Earthquake Engineering*, vol. 33, no. 1, pp. 30–47, 2000.

[9] N. Tarque, L. Candido, G. Camata, and E. Spacone, "Masonry infilled frame structures: state-of-the-art review of numerical modelling," *Earthquake and Structures*, vol. 8, no. 1, pp. 225–251, 2015.

[10] P. G. Asteris, S. T. Antoniou, D. S. Sophianopoulos, and C. Z. Chrysostomou, "Mathematical macromodeling of infilled frames: state of the art," *ASCE Journal of structural engineering*, vol. 137, no. 2, pp. 1508–1517, 2011.

[11] S. V. Polyakov, *On the Interaction Between Masonry Filler Walls and Enclosing Frame When Loading in the Plane of the Wall*, Earthquake Engineering, EERI, Oakland, CA, USA, 1960.

[12] B. Stafford Smith, "Lateral stiffness of infilled frames," *Journal of the Structural Division*, vol. 88, no. 6, pp. 183–199, 1962.

[13] B. Stafford Smith, "Behavior of square infilled frames," *Journal of the Structural Division*, vol. 92, pp. 381–403, 1966.

[14] B. Stafford Smith, "Methods for predicting the lateral stiffness and strength of multi-storey infilled frames," *Building Science*, vol. 2, no. 3, pp. 247–257, 1967.

[15] J. R. Riddington and B. Stafford Smith, "Analysis of infilled frames subject to racking with design recommendations," *The Structural Engineer*, vol. 55, no. 6, pp. 263–268, 1977.

[16] E. Bazan and R. Meli, "Seismic analysis of structures with masonry walls," in *Proceedings of the 7th WCEE*, vol. 5, Springer, Istanbul, Turkey, pp. 633–640, 1980.

[17] A. W. Hendry, *Structural Brickwork*, MacMillan Press, Ltd., London, UK, 1981.

[18] T. Paulay and M. J. N. Priestley, *Seismic Design of Reinforced Concrete and Masonry Buildings*, John Wiley & Sons, Hoboken, NY, USA, 1992.

[19] A. J. Durrani and Y. H. Luo, *Seismic Retrofit of Flat-Slab Buildings with Masonry Infills*, D. P. Abrams, Ed., *in Proceedingsof the NCEER Workshop on Seismic Response ofMasonry Infills*, pp. 1–8, Technical Report NCEER-0004, San Francisco, CA, USA, 1994.

[20] G. Amato, L. Cavaleri, M. Fossetti, and M. Papia, "Infilled frames: influence of vertical load on the equivalent diagonal strut model," in *Proceedings of the 14th World Conference on Earthquake Engineering*, Beijing, China, October 2008.

[21] G. Campione, L. Cavaleri, G. Macaluso, and G. Amato, "Evaluation of infilled frames: an update in-plane-stiffness macro model considering the effects of vertical loads," *Bulletin of Earthquake Engineering*, vol. 13, no. 8, pp. 2265–2281, 2014.

[22] Ministero dei Lavori Pubblici, *Norme Tecniche per L'esecuzione Delle Opere in Cemento Armato Normale e Precompresso e Per le Strutture Metalliche*, Decreto Ministeriale 27 Luglio 1985, Rome, Italy, 1985, in Italian.

[23] D. J. Ewins, *Modal Testing: Theory and Practice*, John Wiley & Sons, Hoboken, NY, USA, 2000.

[24] Vincenzi L., "Identificazione dinamica delle caratteristiche modali e delle proprietà meccaniche di strutture mediante algoritmi di ottimizzazione," Ph.D. dissertation, Department of Civil, Chemical, Environmental and Materials Engineering, University of Bologna, Bologna, Italy, 2007, in Italian.

[25] L. Vincenzi and M. Savoia, "Improving the speed performance of an evolutionary algorithm by a second-order cost function approximation," in *Proceedings of the 2nd International Conference on Engineerign Optimization*, Lisbon, Portugal, September 2010.

[26] V. Thiruvengadam, "On the natural frequencies of infilled frames," *Earthquake Engineering. Structural. Dynamics*, vol. 13, no. 3, pp. 401–419, 1985.

[27] C. Z. Chrysostomou, P. Gergely, and J. F. Abel, "A six-strut model for nonlinear dynamic analysis of steel infilled frames," *International Jounal of Structural. Stability and Dynamics*, vol. 2, no. 3, pp. 335–353, 2002.

[28] W. El-Dakhakhni, M. Elgaaly, and A. Hamid, "Three-strut model for concrete masonry-infilled steel frames," *ASCE*

Journal of Structural Engineering, vol. 129, no. 2, pp. 177–185, 2003.

[29] F. J. Crisafulli and A. J. Carr, "Proposed macro-model for the analysis of infilled frame structures," *Bulletin of the New Zealand Society for Earthquake Engineering*, vol. 40, no. 2, pp. 30–47, 2007.

[30] M. Tondi, M. Bovo, E. Bassoli, L. Vincenzi, and M. Savoia, "Identificazione della rigidezza dei tamponamenti in strutture intelaiate mediante analisi inversa,"in Proceedings of the-ANIDIS Conference, Pistoia, Italy, 2017, in Italian.

[31] M. Tondi, *Innovative model updating procedure for dynamic identification and damage assessment of structures*, Dept. of Civil, Chemical, Environmental and Materials Engineering, University of Bologna, Bologna, Italy, Ph.D. dissertation, 2018.

[32] M. Holmes, "Steel frames with brickwork and concrete infilling," *Proceedings of the Institution of Civil Engineers*, vol. 19, no. 4, pp. 473–478, 1961.

[33] R. J. Mainstone, "On the stiffness and strengths of infilled frames," *Proceedings of the Institution of Civil Engineers*, vol. 49, no. 2, pp. 57–90, 1971.

[34] R. J. Mainstone, *Supplementary Note on the Stiffness and Strengths of Infilled Frames*, Garston, Watford, UK, 1974.

[35] FEMA-274, *NEHRP Commentary on the Guidelines for the Seismic Rehabilitation of Buildings*, FEMA-274, Washington, DC, USA, 1997.

[36] FEMA-306, *Evaluation of Earthquake Damaged Concrete and Masonry Wall Buildings: Basic Procedures Manual*, FEMA-306, Washington, DC, USA, 1998.

[37] T. P. Tassios, "Masonry infill and R/C walls under cyclic actions," in *Proceedings of the 3rd International Symposium on Wall Structures*, Warsaw, Poland, 1984.

[38] L. Te-Chang and K. Kwok-Hung, "Nonlinear behaviour of non-integral infilled frames," *Computers and Strucure*, vol. 18, no. 3, pp. 551–560, 1984.

[39] L. Decanini and G. E. Fantin, "Modelos simplificados de la mamposteria incluida en porticos caracteristicas de rigidez y resistencia lateral en estado limite," *Proceedings of Jornadas Argentinas de Ingegneria Estructural*, vol. 2, pp. 817–836, 1987, in Spanish.

[40] M. Papia and L. Cavaleri, "Effetto irrigidente dei tamponamenti nei telai in c.a." in *Proceedings of the Atti della 2° Conferenza Planetaria "La Sicurezza delle Strutture in Calcestruzzo Armato Sotto Azioni Sismiche Con Riferimento ai Criteri Progettuali di Resistenza al Collasso e di Limitazione del Danno Dell'Eurocodice 8"*, vol. 2, pp. 85–94, Politecnico di Milano, Firenze, Italy, 2001, in Italian.

[41] M. Papia, L. Cavaleri, and M. Fossetti, "Infilled frames: developments in the evaluation of the stiffening effect of infills," *Structural Engineering and Mechanics*, vol. 16, no. 6, pp. 675–693, 2003.

[42] Computers and Structures Inc., 2019, SAP2000 V.21 Software.

[43] A. Stavridis, *Analytical and experimental seismic performance assessment of masonry-infilled RC frames*, Ph.D. thesis, University of California, San Diego, CA, USA, 2009.

[44] R. J. Allemang, "The modal assurance criterion—twenty years of use and abuse, IMAC-XX," in *Proceedings of the 20th International Modal Analysis Conference*, Los Angeles, CA, USA, February 2002.

[45] R. A. Aniendhita and I. Data, "Comparative study on diagonal equivalent methods of masonry infill panel," *AIP Conference Proceedings*, vol. 1855, Article ID 030011, 2017.